Design Considerations for Efficient Binary Megavoltage Photon Detector Structures

Harry Keller, Ralf Hinderer, Marvin Glass, Robert Jeraj, Richard Schmidt, Guang Fang, Jeff Kapatoes, T. Rock Mackie, and Mike L. Corradini

***Abstract*—In this work, Monte Carlo methods are used for the design of highly efficient detector structures for megavoltage X-ray imaging. The detector structures consist of a converter material and an active medium ("binary" detector systems). The novel approach is to impose a spatial structure on the converter material that intersperses the active medium and defines the size of a detector cell. The dimensions of these structures have to be optimized with respect to efficiency and spatial resolution. The results show that the quantum efficiency and detective quantum efficiency at zero frequency of such structures surpasse the efficiency of conventional detector structures using the converter material as a buildup layer and depend on the dimensions of the converter structure and the active medium as well as the materials itself. In general, larger converter structures result in a higher efficiency. The detector signal is proportional to the size of the active medium in the cell. However, the size of the structures are limited by the specifications for the desired spatial resolution.**

***Index Terms*—Binary detector structure, Monte Carlo calculations.**

I. Introduction

In medical physics, photon detectors are extensively used for diagnostic X-ray and CT imaging, nuclear medicine, and, quite recently, radiation therapy of cancer [1], [2]. In modern radiation therapy ever more accurate delivery techniques spur the need for efficient detectors of high-energy photons in the mega-electron volt energy range in order to allow the imaging of the patient during radiation delivery. In particular, in tomotherapy [3], a megavoltage detector is used for both CT imaging and for verifying the dose received by the patients. In order to keep the dose to the patient delivered during imaging as low as possible, efficient radiation detectors are needed. This work aims to develop highly efficient detector structures optimized for the energy range of the photons used in radiation therapy. Monte Carlo calculations play a crucial and invaluable role during the design process of such structures.

Manuscript received November 21, 2001; revised June 17, 2002. This work was supported in part by the U.S. Department of Energy under Grant DE-FG07-ID13918.

H. Keller, R. Hinderer, M. Glass, R. Jeraj, and T. R. Mackie are with the Department of Medical Physics, University of Wisconsin, Madison, WI 53706 USA (e-mail: hkeller@facstaff.wisc.edu).

R. Schmidt, G. Fang, and J. Kapatoes are with Tomotherapy, Inc., Madison, WI 53717 USA (http://www.tomotherapy.com).

M. L. Corradini is with the Department of Engineering Physics and Nuclear Engineering, University of Wisconsin, Madison, WI 53706 USA.

Digital Object Identifier 10.1109/TNS.2002.807880

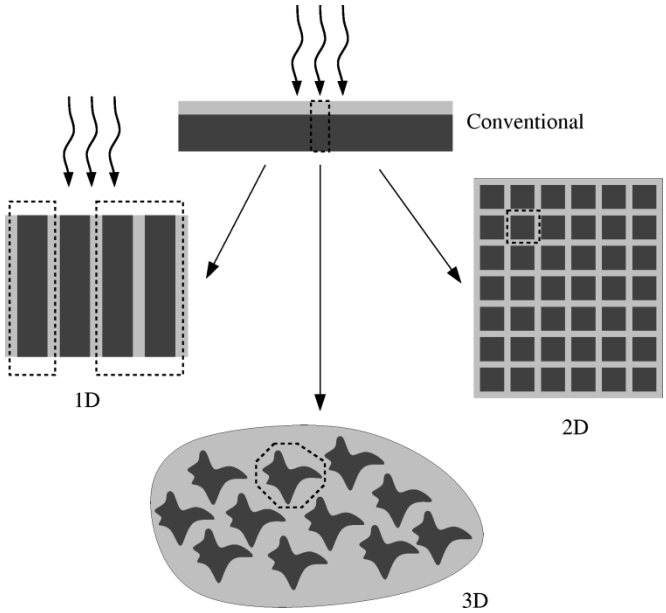

Fig. 1. Binary detector structures. In conventional structures a buildup layer of a converter material (light gray) converts the high-energetic photons to charged particles, which are subsequently detected in the active medium (dark gray). More efficient structures can be constructed by placing thin layers of the converter material in beam direction. The photon beam is hitting the conventional and the 1-D structure from the top. For the 2-D and 3-D case, the photons point into the plane of display. The size of a detector cell (black dashed lines) is imposed by the pixellation of the signal read-out in the conventional structure, but is determined by the converter structure itself for the efficient designs.

II. Materials and Methods

A general binary detector system consists of a converter material and an active medium (cf. Fig. 1). The converter is preferrably a high atomic number and high density material which creates secondary electrons that, in turn, produce a measurable signal in the active medium. The novelty of this approach is to impose a regular or irregular spatial structure on the converter which determines a cell size within the detector system. From each cell the signal can be separately identified. Possible choices for the active medium include a pressurized gas (ionization chamber type), a scintillating material, or a photoconverting amorphous material like a-Se. These binary detector structures differ from conventional detector structures, where a single piece of converter material is usually placed upstream with respect to the active medium, therefore acting as a "buildup" material. Typical detector systems of this kind are the metal plate/phosphor screen systems or the indirect active matrix flat panel devices. Fig. 1 demonstrates the principle

difference between the conventional and the new designs and shows simple one-dimensional (1-D) and two-dimensional (2-D), as well as a general three-dimensional (3-D) detector structure.

Many authors have characterized conventional detector structures for megavoltage radiation [4]–[17]. In this work we focus on the design at the level of signal creation only. Signal collection, signal readout, and the associated readout electronics will not be discussed here. We concentrate on different efficiency measures to characterize the new binary detector systems: signal creation efficiency, quantum (detective) efficiency QE, and detective quantum efficiency at zero frequency DQE (0).

The *signal creation efficiency* is the amount of signal produced in the active medium. Conveniently, in Monte Carlo calculations, the "signal" is the amount of absorbed energy in the active medium. The QE describes the conversion rate from photons to detectable electrons and is the probability per incident photon of producing at least one detectable electron. The third efficiency measure was the DQE at zero frequency DQE(0). It was calculated by using Swank's formula which involves the first and second moments of so-called *absorbed energy distributions (AED)* or spectra of absorbed energies in the active medium of the detector [19]. In the case of a single incident photon energy E_i, DQE(0) is computed from the incident and outgoing signal-to-noise ratios (SNRs) as follows:

$$\mathrm{DQE}(0) = \frac{SNR_{\mathrm{out}}^2}{SNR_{\mathrm{in}}^2} = \frac{SNR_{\mathrm{out}}^2}{\frac{(NE_i)^2}{NE_i^2}} = \frac{1}{N}\frac{M_1^2}{M_2} \qquad (1)$$

where M_1 and M_2 are the first and the second moments of the AED, respectively, and N is the total number of incident photons. In the case of an incident energy spectrum, (1) has to be weighted with the number of photons in each incident energy bin [18]. Using the AEDs, the QE is simply the zeroth moment (or the integral) of the distributions divided by the number of incident photons.

These efficiency measures just described were studied as a function of the cell size and the size of the converter structure in perpendicular direction to the incident X-ray beam. Both the EGS4/BEAM (National Research Council of Canada) and the MCNP4C (Los Alamos National Laboratory) Monte Carlo codes served as the computational tool for the particle transport through the detector structures. In particular, Monte Carlo calculations were done on a linear 1-D array of thin metal plates as the converter (like the 1-D realization in Fig. 1) and a prototype design of a comb-shaped metal converter on an epoxy base with metal shims as collecting electrodes (Fig. 2). The active medium was air. Moreover, the calculations were done for a 4 and 6 MV energy spectrum. These are typical energy spectra produced by two linear accelerators at our institution with nominal acceleration potential of 4 and 6 MeV, respectively. For the linear array structure, the efficiency was also studied for a beam of photons parallel to the plates of the detector and for a divergent beam of photons.

One particular realization of the linear array detector system is the arc-shaped xenon detector used in an earlier generation of CT scanners (GE Medical Systems). Tungsten plates of 320 μm thickness, which subdivide a xenon gas volume of 5 atm pressure in subvolumes of the same dimensions (320 μm), are utilized to collimate the incoming kV photon beam used in CT imaging. In our case (incident MV photon beam), the tungsten plates act as a converter material. The simulations were previously benchmarked against measurements with this CT arc detector by comparing calculated and measured response profiles [18]. Good agreement was found.

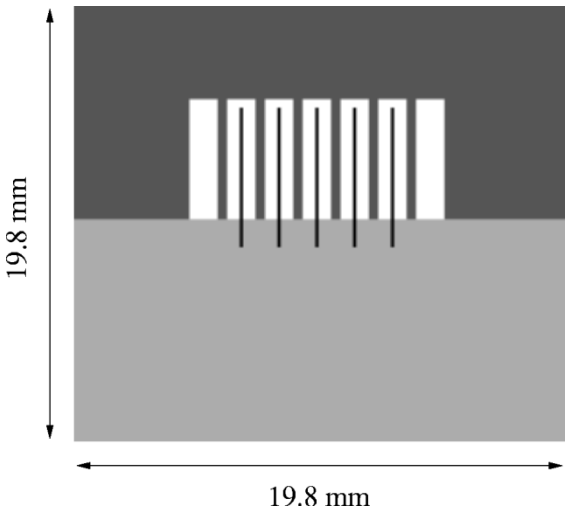

Fig. 2. Schematics of the prototype detector. It consists of a converter structure (top part) attached to an electrical insulator made of epoxy (bottom part). Thin metal shims of 0.13 mm thickness were glued into grooves in the epoxy. The distance between the shims was 1.5 mm. The air cavities were separated by 0.38 mm thick converter plates extending from the top part to the epoxy base. The detector extends 4 cm in the direction perpendicular to the paper plane. To read out the ionization charges from the air cavities a high voltage is applied to the converter structure and the collecting electrodes are connected to an electrometer.

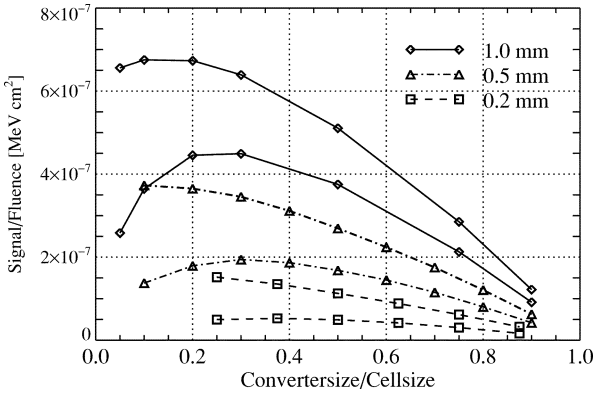

Fig. 3. Signal creation efficiency for the 1-D linear array structure as a function of the ratio between converter size and cell size (the reciprocal fill factor). The "signal" is the absorbed energy in one of the central gas cavities. In this particular case, the converter plates were made of tungsten and the gas was air. The different line styles of the curves represent calculations for different fixed cell sizes, which is indicated in the legend. The cell size is the distance between two tungsten plates. For each cell size, the signal was scored for an incident broad beam and for an incident narrow beam of 6 MV energy covering the central cell. Hence, for comparison between the different cell sizes, the signal was normalized to the incident photon fluence. The curves showing the larger signal for a given fill factor is the one for the incident broad beam. The ratio between the curves for a given cell size and fill factor is a measure for the cross talk or scatter within the detector structure.

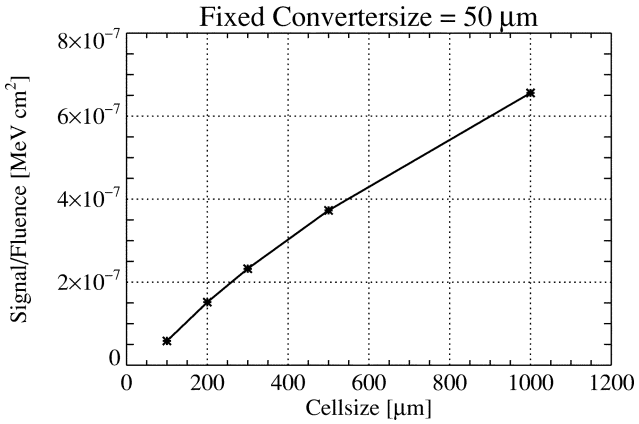

Fig. 4. Absorbed energy per incident photon fluence from Fig. 3 as a function of cell size for fixed size of the tungsten plates.

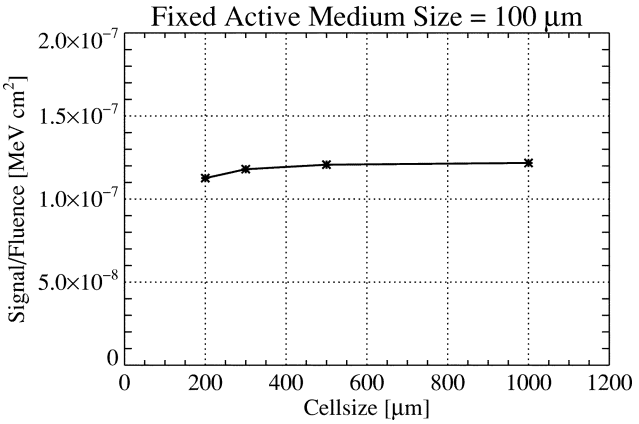

Fig. 5. Absorbed energy per incident photon fluence from Fig. 3 as a function of cell size for fixed size of the gap between the plates.

III. Results and Discussion

A. Signal Creation Efficiency

For a linear tungsten plate-air array structure, the signal creation efficiency was investigated as a function of variable converter plate thickness and variable cell size. The absorbed energy was scored in a central air cavity of the array. The results are shown in Figs. 3–5. Referring to Fig. 3, for a narrow beam covering only one detector cell, there exists a distinct maximum in the collected signal for a certain plate thickness for a given cell size. For thinner plates, fewer secondary electrons are produced, causing the signal to drop. For thicker plates, the signal collecting volume of the active medium decreases, which also leads to a drop in signal. Irradiating the entire detector with a broad photon beam leads to a considerable contribution of scatter signal (cross talk) to the central cell, which increases with decreasing plate thickness. Hence, the ratio between the narrow beam signal and the scatter signal is monotonically increasing with plate thickness. All these observations are valid for all the shown cell sizes. Summarizing the results of Fig. 3, smaller plates generally produce a larger amount of signal but show larger cross talk.

In order to highlight the importance of the dimensions of the converter material and the active medium to the amount of created signal in the linear structure, Fig. 4 shows the results of Fig. 3 for a fixed converter plate thickness of 50 μm and Fig. 5 for a fixed size of the air gap of 100 μm between the plates. The results show, that the produced signal is to first order only proportional to the size of the active medium and almost independent of the dimension of the converter plates. The first point is not surprising and simply follows from the fact that the amount of absorbed energy is proportional to the pathlength of the electrons crossing the medium. The proportionality holds as long as the dimensions of the medium are shorter than the pathlengths of the electrons. The second point is a consequence of the aforementioned proportionality and that, for thicker plates, the increasing production of electrons is countered by the decreasing cross talk.

The total absorbed energy in the seven air cavities of the prototype detector was studied for three different converter materials (aluminum, copper, and tungsten), two photon beam energies (4 MV and 6 MV) and two different thicknesses of the detector in beam direction (1 cm and 4 cm). The results are shown in Fig. 6. First, the results are most sensitive to a change in detector thickness. For aluminum, the signal produced in the thick detector (4 cm) is approximately 4 times larger than in the thin detector (1 cm), for copper 3.3 times and for tungsten 2.5 times. This is a direct consequence of the increased attenuation of the photon beam with larger material thickness. Second, for the thin detector, the total signal is increasing with increasing material density, whereas for the thick detector, the total signal is decreasing with increasing material density. This result is not surprising considering the two opposing influences on the amount of absorbed energy: with increasing material density the number of photon interactions is increasing but at the same time, the pathlengths of the produced secondary particles is decreasing, therefore reducing the events, where energy from the same electron is deposited in more than one air cavity (cross talk). For the thin detector, the increased number of photon interactions outweighs the decrease of the cross talk, whereas for the thick detector this is reversed. This highlights, that not only efficiency parameters should be considered in the design of such detectors but also resolution parameters, which are determined by the amount of cross talk.

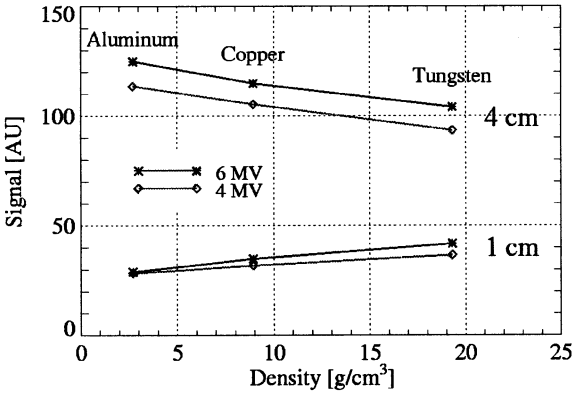

Fig. 6. Total absorbed energy (signal in arbitrary units) in the seven air cavities of the prototype detector for different converter material. The label "4 cm" refers to the thick detector; "1 cm" to the thin detector.

Furthermore, Fig. 6 shows, that the amount of signal is dependent on the beam energy. For the thick detector, the signal was about 10% higher for the 6 MV photon energy spectrum

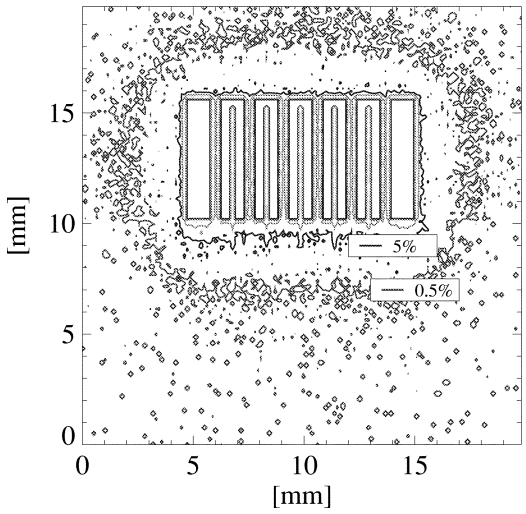

Fig. 7. Contour plot of the relative contribution (importance) to the absorbed energy in the active medium of the 4 cm thick prototype detector for 10^8 photon histories. The simulation geometry is shown in Fig. 2. The incoming 4 MV photon beam is pointing into the plane of display. The converter structure is tungsten. The absorbed energy in the air cavities was mapped back to the location of the first interaction of the photon. The two innermost contour lines represent the 20% and the 50% contribution level, respectively. In this case the contributions from each material to the absorbed energy in air was: tungsten 58%, steel shims 18%, epoxy 23%, and air 1%.

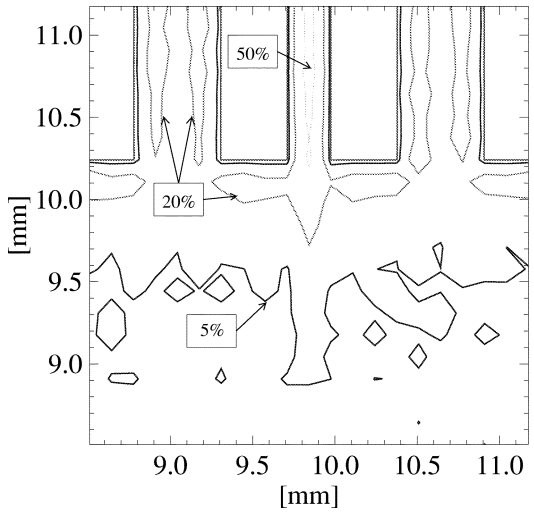

Fig. 8. Central part of Fig. 7, showing the bottom part of the central air cavity split by the central collecting electrode.

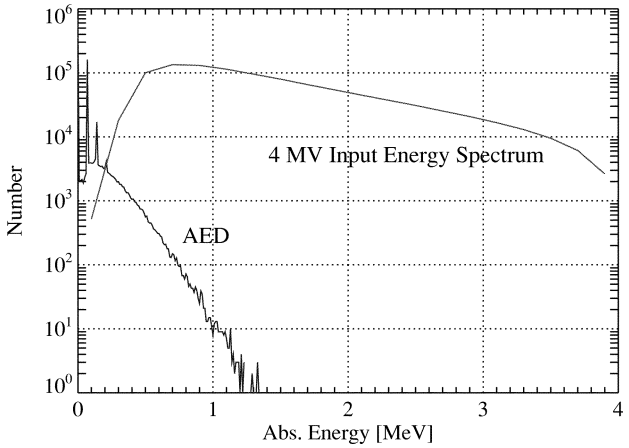

Fig. 9. 4 MV input energy spectrum and corresponding absorbed energy distribution of the linear tungsten plate-xenon gas array (CT detector). The peaks in the AED are due to photoeffects in xenon of K-edge X-rays from tungsten. From the first and second moments of these distributions the detective quantum efficiency at zero frequency DQE(0) is calculated according to Swank's formula (1).

compared with the 4 MV energy spectrum. The thin detector showed only a modest difference between the two photon beam qualities.

In order to support design considerations for the prototype and to study the importance of the signal contribution from different materials, spatial maps of the origin of the absorbed energy (so-called "importance maps") were calculated. This was done by scoring the energy not at the location of its absorption, but at the location of the first interaction of the first photon in the history. One example of such a map with tungsten as the converter material is shown in Figs. 7 and 8. From the figures, it is clear, that the vast majority of the signal originates in the immediate vicinity of the air cavities and can be attributed to compton electrons. It is clearly seen from the 5% contour line in Fig. 7, that the range of these electrons is larger in the epoxy than in the tungsten converter. A low percentage of the signal is originating from locations farther away than the electron range and is due to multiple compton events.

The importance maps provide information to optimize dimensions and choice of materials at once.

B. QE and DQE

Fig. 9 shows an example of an absorbed energy distribution within the CT arc detector for an incident 4 MV photon beam. The AED is heavily weighted toward low energies. The largest amount of energy absorbed in the detector from a single photon is about 1.3 MeV.

The results for QE and DQE(0) for the CT arc detector are shown in Table I. The cell size was fixed at 640 μm, which is the distance between the plates in the arc-shaped CT detector. From the table, it is seen, that the tungsten plates are much more efficient than the aluminum plates and that the divergent photon beam causes even more photons to interact. This is obvious, as the plate surface exposed to the radiation is greatly increased for the divergent photon beam. In comparison, these numbers reach at most only 4% to 5% for conventional detector structures. An additional calculation showed, that the efficiency numbers in Table I are even larger for thicker plates.

An additional calculation showed, that the efficiency numbers in Table I are even larger for thicker plates.

An important remark is appropriate. It appears, that thicker plates are more convenient in terms of QE, DQE(0), and cross talk. However, as seen above, the signal creation efficiency and, therefore, the SNR is much smaller than for thinner plates. Therefore, for a given SNR, thicker plates produce less cross talk, allowing a larger signal transfer at higher spatial frequency and therefore a higher resolution, but produce less signal. On the other hand, thicker plates are associated with a larger cell size which deteriorates resolution. Consequently, for a given SNR, the thickness of the converter plates has to be optimized with respect to the signal transfer at all spatial frequencies (modulation transfer function). This will also be dependent

TABLE I
QE AND DQE(0) (IN %) FOR THE 1-D-ARRAY DETECTOR STRUCTURE WITH 5 ATM XENON GAS AS THE ACTIVE MEDIUM. THE FIRST COLUMN INDICATES THE PLATE MATERIAL USED IN THE CALCULATION. "PARALLEL" DENOTES A VECTORIELL PHOTON FLUENCE PARALLEL TO THE PLATES OF THE ARRAY, "DIVERGENT" DENOTES A DIVERGENT BEAM OF PHOTONS. THE CELL SIZE WAS 640 μm AND THE PLATE THICKNESS 320 μm

X-ray Energy/ Plate material	X-ray beam	QE [%]	DQE(0) [%]
4 MV/Al	Parallel	9.5	6.8
4 MV/Al	Divergent	9.9	7.1
4 MV/W	Parallel	29.2	20.4
4 MV/W	Divergent	44.4	29.3
6 MV/W	Parallel	39.8	31.1
6 MV/W	Divergent	46.4	35.7

on the kind of materials used. All these investigations will be presented in future work.

IV. CONCLUSION

A binary detector design with a structured high-density converter material is a promising candidate for a very efficient radiation detector.

Compared to conventional technologies the efficiency numbers are one order of magnitude higher. However, the choice of converter materials and the dimensions of the detector have to be optimized within the limits imposed by the specifications for the spatial resolution.

REFERENCES

[1] P. Munro, "Portal imaging technology: Past, present and future," *Semin. Rad. Oncol.*, vol. 5, pp. 115–133, 1995.

[2] A. L. Boyer, L. Antonuk, A. Fenster, M. van Herk, H. Meertens, P. Munro, L. E. Reinstein, and J. Wong, "A review of electronic portal imaging devices (EPID's)," *Med. Phys.*, vol. 19, pp. 1–16, 1992.

[3] G. H. Olivera, D. M. Shepard, K. Ruchala, J. S. Aldridge, J. M. Kapatoes, E. E. Fitchard, P. J. Reckwerdt, G. Fang, J. Balog, J. Zachman, and T. R. Mackie, "Tomotherapy," in *Modern Technology of Radiation Oncology*, J. Van Dyk, Ed. Madison, WI: Medical Phys., 1999, pp. 521–587.

[4] T. Radcliffe, G. Barnea, B. Wowk, R. Rajapakshe, and S. Shalev, "Monte Carlo optimization of metal/phosphor screens at megavoltage energies," *Med. Phys.*, vol. 20, pp. 1161–1169, 1993.

[5] B. Wowk, T. Radcliffe, K. Leszczynski, S. Shalev, and R. Rajapakshe, "Optimization of metal/phosphor screens for on-line portal imaging," *Med. Phys.*, vol. 21, pp. 227–235, 1994.

[6] H. Wang, B. G. Fallone, and T. Falco, "Monte Carlo simulations of a metal/a-Se portal detector," *Radiol. Oncol.*, vol. 30, pp. 291–297, 1996.

[7] J.-P. Bissonnette, I. A. Cunningham, D. A. Jaffray, A. Fenster, and P. Munro, "A quantum accounting and detective quantum efficiency analysis for video-based portal imaging," *Med. Phys.*, vol. 24, pp. 815–826, 1997.

[8] J. P. Bissonnette, I. A. Cunningham, and P. Munro, "Optimal phosphor thickness for portal imaging," *Med. Phys.*, vol. 24, pp. 803–814, 1997.

[9] M. Lachaine and B. G. Fallone, "Monte Carlo detective quantum efficiency and scatter studies of a metal/ a-Se portal detector," *Med. Phys.*, vol. 25, pp. 1186–1194, 1998.

[10] T. Falco and B. G. Fallone, "Characteristics of metal-plate/film detectors at therapy energies: I. Modulation transfer function," *Med. Phys.*, vol. 25, pp. 2455–2462, 1998.

[11] ——, "Characteristics of metal-plate/film detectors at therapy energies: II. Detective quantum efficiency," *Med. Phys.*, vol. 25, pp. 2463–2468, 1998.

[12] M. A. Mosleh-Shirazi, W. Swindell, and P. M. Evans, "Optimization of the scintillation detector in a combined 3D megavoltage CT scanner and portal imager," *Med. Phys.*, vol. 25, pp. 1880–1890, 1998.

[13] D. Mah, J. A. Rawlinson, and J. A. Rowlands, "Detective quantum efficiency of an amorphous selenium detector to megavoltage radiation," *Phys. Med. Biol.*, vol. 44, pp. 1369–1384, 1999.

[14] C. Kausch, B. Schreiber, F. Kreuder, R. Schmidt, and O. Dössel, "Monte Carlo simulations of the imaging performance of metal/phosphor screens used in radiotherapy," *Med. Phys.*, vol. 26, pp. 2113–2124, 1999.

[15] C. Kausch, F. Cremers, D. Albers, R. Schmidt, and B. Schreiber, "Monte Carlo simulation of a prototype photodetector used in radiotherapy," *Nucl. Instrum. Methods A*, vol. 442, pp. 53–57, 2000.

[16] M. Lachaine, E. Fourkal, and B. G. Fallone, "Detective quantum efficiency of a direct-detection active matrix flat panel imager," *Med. Phys.*, vol. 28, pp. 1363–1372, 2001.

[17] ——, "Investigation into the physical characteristics of active matrix flat panel imagers for radiotherapy," *Med. Phys.*, vol. 28, pp. 1689–1695, 2001.

[18] H. Keller, M. Glass, R. Hinderer, K. Ruchala, R. Jeraj, G. Olivera, and T. R. Mackie, "Monte Carlo study of a highly efficient gas ionization detector for megavoltage imaging and image-guided radiotherapy," *Med. Phys.*, vol. 29, pp. 165–175, 2002.

[19] R. Swank, "Absorption and noise in X-ray phosphors," *J. Appl. Phys.*, vol. 44, pp. 4199–4203, 1973.